Bioorganic & Medicinal Chemistry 21 (2013) 7011–7017

Contents lists available at ScienceDirect

Bioorganic & Medicinal Chemistry

journal homepage: www.elsevier.com/locate/bmc

Antibody-catalyzed decarboxylation and aldol reactions using a primary amine molecule as a functionalized small nonprotein component

Fumihiro Ishikawa [a,b], Kouki Uno [a], Masao Nishikawa [a], Takeshi Tsumuraya [a], Ikuo Fujii [a,*]

[a] Department of Biological Science, Graduate School of Science, Osaka Prefecture University, 1-1 Gakuen-cho, Naka-ku, Sakai, Osaka 599-8531, Japan
[b] Department of System Chemotherapy and Molecular Science, Division of Bioinformatics and Chemical Genomics, Graduate School of Pharmaceutical Sciences, Kyoto University, Sakyo, Kyoto 606-8501, Japan

ARTICLE INFO

Article history:
Received 11 August 2013
Revised 5 September 2013
Accepted 6 September 2013
Available online 19 September 2013

Keywords:
Catalytic antibody
Decarboxylation reaction
Regioselective aldol reactions
Enamine mechanism

ABSTRACT

Catalytic antibody 27C1 bears binding sites for both a substrate- and a functionalized small nonprotein component in the active site. We investigated the possibility of exploiting imine and enamine intermediates using a primary amine molecule into the active site of antibody 27C1. The antibody catalyzed β-keto acid decarboxylation with a rate enhancement ($k_{cat}/K_m/k_{uncat}$) of 140,000, as well as highly regioselective cross-aldol reactions of ketones and *p*-nitrobenzaldehyde. These studies provide new strategies for the generation of catalytic antibodies possessing binding sites for functionalized components.

1. Introduction

The study of amine-catalyzed decarboxylation and aldol reactions remains a special area of research in synthetic chemistry, bioorganic chemistry and enzymology.[1–4] A number of elegant enzymatic studies elucidated the mechanism by which acetoacetate decarboxylase catalyzes the decarboxylation of acetoacetic acid.[5–14] These studies demonstrated that the reaction proceeds by the formation of a Schiff base between the ε-amino group of a lysine residue in the enzyme and acetoacetate, followed by decarboxylation to form an enamine, which is then tautomerized to a Schiff base and subsequently hydrolyzed to release acetone and the free enzyme. The imine and enamine intermediates developed along the reaction catalyzed by acetoacetate decarboxylase are also found along the reaction coordinate of reactions between aldolases and aldol donors. In fact, natural class I aldolases and the programmed catalytic antibodies 38C2 and 33F12, which both have an active-site lysine residue are bifunctional catalysts. In addition to catalyzing the decarboxylation of β-keto acids, they also catalyze the aldol reaction of aldehydes and ketones.[15–19] Unlike natural enzymes, antibodies 38C2 and 33F12 were found to accept a variety of ketones and aldehydes as aldol donors and acceptors to achieve regio- and enantioselevtive aldol reactions.[20] The application of catalytic antibodies has thus yielded numerous efficient syntheses of stereochemically complex molecules.[21–24]

Recently, we developed catalytic antibody 27C1, which bears an antigen-combining site that functions as an apoprotein for binding functionalized small nonprotein components.[25] This antibody was elicited by immunization with the haptenic phosphonate diester **1**. The *p*-nitrophenyl and *N*-acetylphenyl groups in hapten **1** were designed to elicit binding sites for the substrate and the functionalized component, respectively, in the antigen-combining site (Fig. 1a). With a simple exchange of the functionalized component, antibody 27C1 is capable of catalyzing a wide range of chemical transformations including acyl-transfer, β-elimination, decarboxylation, and aldol reactions. Particularly, antibody 27C1 catalyzed the aldol reaction of acetone and *p*-nitrobenzaldehyde **4** in the presence of the functionalized component **2** (Fig. 1b).[25] Catalysis by 27C1 was efficient compared with the non-catalyzed reaction, showing a rate enhancement $[(k_{cat}/K_m$ **4**$)/k_{uncat}$ of 4.4×10^4 (27C1: $k_{cat} = 25.8\ min^{-1}$, K_m for **4** = 958 μM, K_m for **2** = 67 mM). In the aldol reaction, the direct precursor of the enamine is an imminium ion; the presence of the imminium ion was established by isolation of the reduction product following $NaBH_4$ treatment. Examination of enamine formation with acetone and amine **2** in the presence of $NaBH_4$ showed that antibody 27C1 catalyzed the formation of an isopropylation product, providing evidence for an enamine mechanism for the antibody-catalyzed reaction. This enamine formation was inhibited by addition of hapten **1**, showing that the enamine was formed in the antigen-combining site. In this

* Corresponding author. Tel./fax: +81 72 254 9834.
E-mail address: fujii@b.s.osakafu-u.ac.jp (I. Fujii).

0968-0896/$ - see front matter © 2013 Elsevier Ltd. All rights reserved.
http://dx.doi.org/10.1016/j.bmc.2013.09.015

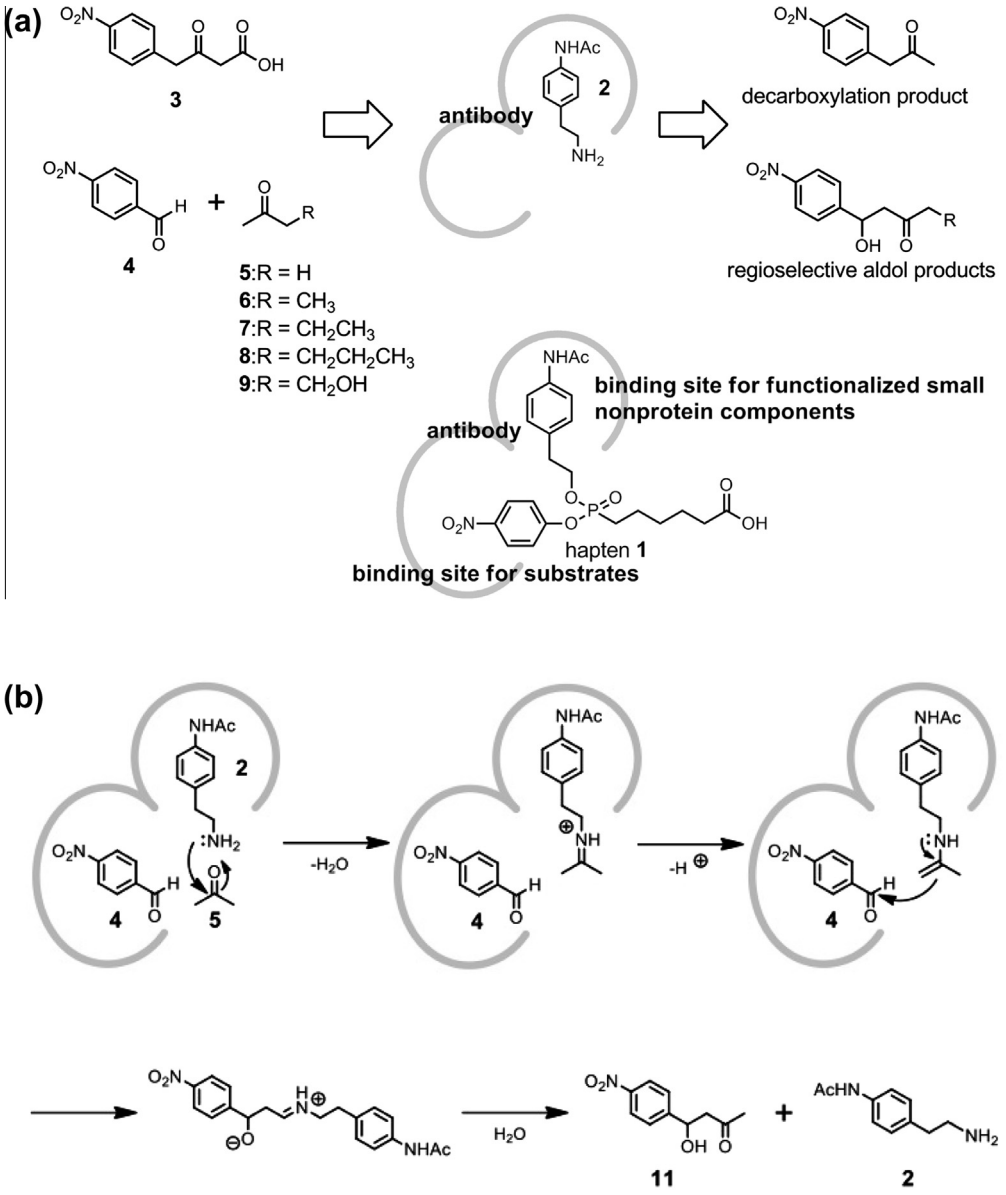

Figure 1. (a) Decarboxylation and aldol reactions catalyzed by antibody 27C1 and structure of the immunized hapten **1**. (b) The mechanism of the antibody-catalyzed aldol reaction.

work, we have investigated the possibility of exploiting the common imine and enamine intermediates using a primary amine molecule in the antibody-combining site. The primary amine mimics a lysine residue correctly aligned in the active sites of natural enzymes and the catalytic antibodies 38C2 and 33F12. Here, we demonstrate the utility of the amine molecule for catalyzing the decarboxylation of a β-keto acid, as well as aldol reactions using structurally related aldol donors (Fig. 1a).

2. Results

2.1. Decarboxylation reaction

Antibody 27C1 catalyzed the decarboxylation reaction of β-keto acid **3** to afford (*p*-nitrophenyl)acetone. Lineweaver–Burk plots were constructed by holding the either the substrate or the functionalized component constant while varying the concentration of the other (Fig. 2). The slopes and *y*-intercepts obtained from this analysis were replotted as a function of substrate or functionalized component concentration to provide the true maximum rate V_{max} (12.9 μM min^{-1}) and the Michaelis constant, K_m (Fig. 2). The uncatalyzed reaction of β-keto acid **3** with amine **2** was monitored by high performance liquid chromatography (HPLC) as a pseudo-first-order reaction. Product formation was assayed from 0 to 540 min and the second-order rate constant was calculated ($k_{uncat} = 4.55 \times 10^{-6}$ mM^{-1} min^{-1}). The k_{uncat} can be considered as k_{amine}, amine **2**-catalyzed decarboxylation of β-keto acid **3**. Catalysis by 27C1 was remarkably efficient compared with the non-catalyzed reaction, showing a large rate enhancement [(k_{cat}/K_m **3**)/k_{uncat} (the relative efficiencies over amine catalysis)] of 140,000; (k_{cat} (per binding site) = 1.29 min^{-1}, K_m (for **3**) = 2.1 mM, K_m (for **2**) = 6.7 mM, pH 8.0) (Fig. 2).

2.2. Cross-aldol reactions

To demonstrate the versatility and define the scope of antibody 27C1 for the cross-aldol reactions, we tested a variety of commercially available ketones **5**–**10** as donors and *p*-nitrobenzaldehyde

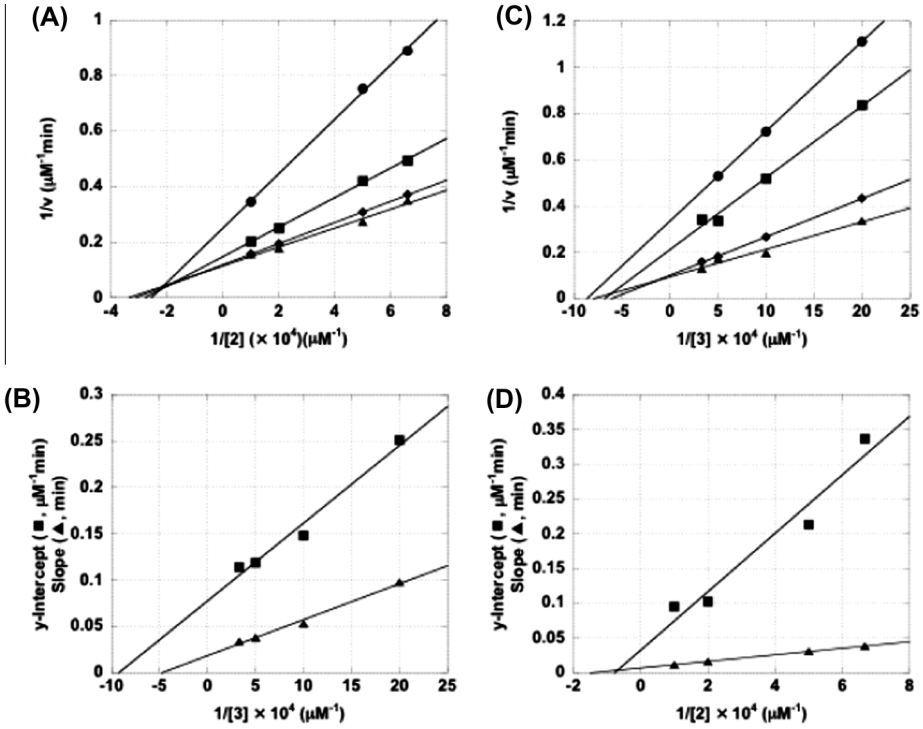

Figure 2. (A) Lineweaver–Burk plot with **3** held at four fixed concentrations while **2** was varied over concentrations ranging from 1.5 to 10 mM (●, [**3**] = 0.5 mM; ■, [**3**] = 1 mM; ♦, [**3**] = 2 mM; ▲, [**3**] = 3 mM); *v*, velocity. (B) Replot of the *y*-intercepts and slopes of the Lineweaver–Burk plot as a function of $[\mathbf{3}]^{-1}$. (C) An analogous Lineweaver–Burk plot was constructed with **2** held at four fixed concentrations while **3** was varied over concentrations from 0.5 to 3 mM (●, [**2**] = 1.5 mM; ■, [**2**] = 2 mM; ♦, [**2**] = 5 mM; ▲, [**2**] = 10 mM). (D) An analogous plot was constructed to provide the kinetic constants for **2**. The reaction mixtures contained 5 μM antibody 27C1, 10% (v/v) DMSO, and 50 mM Tris–HCl pH 8.0. The mixtures were incubated at 25 °C. All kinetic assays were measured in duplicate.

4 as an acceptor (Fig. 1a and Table 1). Aldehyde **4** was chosen as the standard acceptor because, like hapten **1**, it bears a *p*-nitrophenyl group and should be specifically recognized by the antibody. To assign regioselectivity, the aldol products were synthesized by standard methods (see Section 5). To compare the reactivity of aldol donors, we determined specific rates for the antibody-catalyzed reactions under the following defined conditions: 5% donor, 1 mM of *p*-nitrobenzaldehyde **4**, 10 mM of the primary amine **2**, and 10 μM of 27C1 in 50 mM Tris–HCl pH 8.0. As shown in Table 1, a variety of different ketones underwent the antibody-catalyzed aldol reactions with aldehyde **4**, as proven by comparison of the HPLC retention times of the aldol products with those of independently chemically synthesized standards: aliphatic open chain (acetone, 2-butanone, 2-pentanone, and 2-hexanone), and functionalized open chain (4-hydroxy-2-butanone). All antibody-catalyzed aldol reactions were inhibited by addition of hapten **1** or removal of functionalized molecule **2**. Cyclobutanone was not accepted by antibody 27C1, presumably because of its bulkiness.

2.3. Regioselectivity of the aldol reactions

We set out to study the degree of regiocontrol that antibody 27C1 could exercise on the aldol reactions. For all experiments, the reaction products were proven by comparison of the retention times of the products and independently chemically synthesized standards using HPLC. We performed the reactions under the following defined conditions: 5% donor, 500 mM **4**, 500 mM amine **2**, and 10 mM antibody in 50 mM Tris–HCl pH 8.0 at 25 °C. Control experiments revealed that, in the absence of antibody, the products were the *syn* and *anti* stereoisomers resulting from an addition of the more substituted carbon of 2-butanone, 2-pentanone, and 2-hexanone to the aldehyde (Table 2). When 4-hydroxy-2-butanone was used as the donor, the products were a mixture of the linear isomer **15** and branched isomer **15a** (44:56) (Table 2). These results suggest that under these conditions, the non-catalyzed reactions are exclusively under thermodynamic control. Using the antibody, we found that the product distribution is a function of the catalyst, the acceptor and the donor. Antibody 27C1 predominantly afforded the linear regioisomers. The reaction of 2-butanone (**6**) with **4** produced the linear isomer **12** exclusively (**12**:**12a**, >99). The reaction of 2-pentanone (**7**) with **4** predominantly produced the linear isomer **13** (**13**:**13a**, 90:10). The reaction of 4-hydroxy-2-butanone (**9**) with **4** exclusively provided linear isomer **15** (**15**:**15a**, >99). The reaction of 2-hexanone (**8**) with **4** was moderately regioselective, producing a mixture of the linear and branched isomers **14** and **14a** (**14**:**14a**, 62:38).

3. Discussion

The catalytic efficiency of antibody 27C1 as a decarboxylase can be assessed by comparing decarboxylation reactions catalyzed by the antibody, simple amines,[26–29] catalytic antibodies 38C2 and 33F12,[18] and the enzyme acetoacetate decarboxylase (AAD).[5–13,30] The most effective amine catalyst for the decarboxylation of acetoacetate is aminoacetonitrile, AAN.[28] This amine molecule has been used as a model for AAD-catalyzed decarboxylations because its p*K*a value approximates that of the active-site lysine of AAD. The rate of AAD-catalyzed decarboxylation of acetoacetate is 156 times the rate of decarboxylation catalyzed by AAN, suggesting that most of AAD's catalytic ability can be attributed to imine formation with the amino group of the active site lysine.[27,30] AAD-, 38C2-, and 33F12-catalyzed decarboxylation reactions proceeded in single-substrate manner. In contrast, antibody 27C1 catalyzed reactions between two substrates (β-keto acid **3** and amine **2**). Thus, we could not directly compare the rate enhancement, k_{cat}/k_{uncat} for 27C1-catalyzed decarboxylation reaction with those of

Table 1
Donor promiscuity of antibody 27C1: specific rates (μmol product h^{-1} $μmol^{-1}$ antibody) for antibody-catalyzed cross-aldol reactions of a variety of ketones with *p*-nitrobenzaldehyde **4** under the following defined conditions: 5% donor, 1 mM **4**, 10 mM **2**, and 10 μM antibody. R = *p*-nitrophenyl

Donor	Product(s)	Specific rate
 **5**	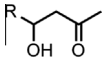 **11**	55.0
 **6**	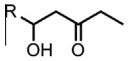 **12**	7.6
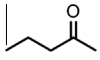 **7**	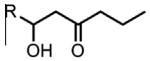 **13**	6.6
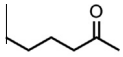 **8**	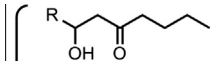 **14** 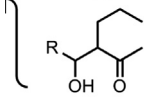 **14a**	0.2[a]
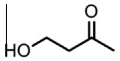 **9**	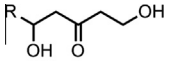 **15**	22.1
 **10**	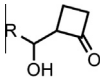 **16**	nd[b]

All kinetic assays were measured in duplicate.
[a] Specific rate was determined with 2.5 mM **2**.
[b] Not determined.

natural enzyme and specialized catalytic antibodies. For ease, we evaluated the relative efficiencies over amine catalysis, $k_{cat}/K_m/k_{amine}$. The large rate enhancement [$(k_{cat}/K_m$ **3**$)/k_{amine}$] of 140,000 for 27C1-catalyzed decarboxylation is comparable to the rate acceleration for 38C2-catalyzed decarboxylation of structurally related β-keto acids (Table 3). This result suggests that the primary amine **2** in the antigen-combining site of 27C1 has a pK_a value similar to those of the active-site lysines of AAD and 38C2. The antibodies 38C2 and 33F12 provide a 10,000–25,000-fold rate enhancement ($k_{cat}/K_m/k_{amine}$) for the decarboxylation of structurally related β-keto acid. These catalytic activities are 10-fold lower than that of 27C1 (Table 3). The effectiveness of 27C1 results from the higher effective molarity of the active-site amine molecule (2.8×10^2 M) compared with the active-site lysines of 38C2 (24 M) and 33F12 (18 M) (Table 3). Efficient decarboxylation in antibody 27C1 presumably reflects the entropic advantage derived from correctly alignment of the perturbed amine molecule with the carbonyl carbon of β-keto acid **3**.

Antibody 27C1 is capable of accepting a variety of ketones for intermolecular aldol reactions with *p*-nitrobenzaldehyde. Previous biochemical studies of this catalyst suggested an enamine mechanism shared with the natural class I aldolase enzymes except for the presence of a primary amine molecule instead of a lysine residue. A primary amine molecule in the antigen-combining site functions as a chemically unique lysine residue bearing an ε-amino group, which has a highly perturbed p*K*a allowing for efficient amine-based catalysis under conditions where a more typical amine would be protonated and ineffective in this chemistry. Amang the aldol reactions, the reaction involving 4-hydroxy-2-butanone as the donor was significantly more efficient than those involving the other ketones except acetone. Neverthless, these studies suggest that the donor specificity of 27C1 is broad, albeit limited to open-chain ketones. These experiments also indicate an active site geometry which strictly recognizes substitutions such as cyclobutanone along with the designed hapten molecule. The donor specificity may reflect the alkyl linker moiety in the hapten, which generates antibody catalysts with broad substrate specificity.[31] We found that unlike antibodies 38C2 and 33F12,[18] antibody 27C1 favored formation of the linear regioisomer regardless of the structure of the aldol donors. The reactions involving ketones **6**–**9** with *p*-nitrobenzaldehyde (**4**) all provided predominantly or exclusively the aldol product resulting from the less substituted carbon. Although antibody 27C1 preferentially catalyzed regioselective formation of the linear isomer, the antibody-catalyzed aldol reactions gave no enantiomeric excess (ee). When acetone was the aldol donor substrate in the *p*-nitrobenzaldehyde–ketone crossed aldol reaction, the product was a racemic

Table 2
Regioselectivity of antibody-catalyzed cross-aldol reactions of a variety of ketones (**6**–**9**) with *p*-nitrobenzaldehyde **4**

Donor	Product (s)	Regioselectivity	
		Uncatalysed	Catalyzed
 **6**	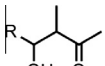 **12a** 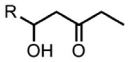 **12**	96:4	<99
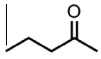 **7**	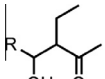 **13a** 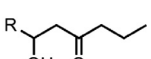 **13**	83:17	10:90
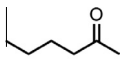 **8**	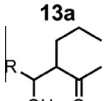 **14a** 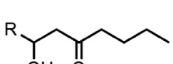 **14**	92:8	38:62
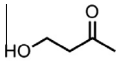 **9**	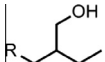 **15a** 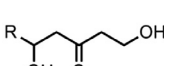 **15**	56:44	<99

All kinetic assays were measured in duplicate.

Table 3
Kinetic parameters for antibody-catalyzed decarboxylation reactions

Catalyst	k_{cat}/k_{uncat}	$k_{cat}/K_m/k_{uncat}$	k_{cat}/k_{amine} (M)
AAD	5.2×10^9 [a]	9.5×10^6 [b]	7.8×10^7
38C2	1.4×10^4 [c]	2.5×10^4 [c]	23.8[c]
33F12	1.1×10^4 [c]	1.0×10^4 [c]	18.1[c]
27C1		1.4×10^5	2.8×10^2

[a] k_{cat} and K_m of acetoacetate decarboxylase (AAD)-catalyzed decarboxylation of acetoacetate from Highbarger et al.,[30] k_{uncat} from Westheimer.[14]
[b] k_{amine}, aminoacetonitrile-catalyzed decarboxylation of acetoacetate from Westheimer.[14]
[c] k_{cat} and K_m of the 38C2 and 33F12-catalyzed decarboxylation from Björnestedt et al.[19] Amine = phenylalanine ethyl ester for 38C2 and 33F12.

mixture of **11**. When 2-butanone was used as the donor substrate, the aldol product possessed the *R*-configuration with moderate 48% ee. These results suggest that the enamine formed by the reaction between **2** and 2-butanone attacks on both the *re*- and *si*-faces of *p*-nitrobenzaldehyde owing to the lack of additional interactions to constrain the binding mode of the acceptor molecule in the antigen-combining site. Further insight into the low enantioselectivity of 27C1 will be provided by the X-ray crystal structure.

4. Conclusion

These studies highlight the ability of the antigen-combining site of antibody 27C1, elicited by immunization with the haptenic phosphonate diester **1**, to function as an apoproteins for binding functionalized small nonprotein components. The programming of the binding site for the functionalized component involved in catalysis constitutes a unique feature of this approach and is as significant as the use of transition state analogs to induce catalytic antibodies.[32] Ultimately, one would wish to combine both methods, enabling the experimenter to control both the global aspects and the mechanistic details of the reaction. This approach offers significant advantages over other methods for producing 'specialized' catalytic antibodies. It is possible to introduce additional catalytic components (transition state stabilization, acid, and base catalysis) by mutations of amino acids in the active site. Although 27C1 is the best catalytic antibody for decarboxylation, the rate enhancement $[(k_{cat}/K_m)/k_{uncat} = 140{,}000]$ for the 27C1-catalyzed decarboxylation of **3** is 10^4-fold lower than that reported for acetoacetate decarboxylase (Table 3). The large rate acceleration of 27C1 may shed light on the catalytic power of the amine molecule by the proximity effect responsible for the enormous rate enhancements observed for natural enzymes. As natural enzymes display the rate enhancements of 10^6–10^{17} by a combination of several catalytic mechanisms, it is expected that additional rate accelerations will be realized by introducing not only functionalized small molecules but also specific amino acid residues that function as transition-state stabilization and general acid–base catalysis into the antigen-combining site, using phage-displayed libraries[33] or site-directed mutagenesis.[34] The low enantioselectivity of aldol reactions could be improved by altering the binding mode of aldol donor and acceptor substrates through site-directed mutagenesis. Our results demonstrate that antibodies incorporating newly devised components acting as 'chemical teeth' will enlarge the scope and broaden the reaction boundaries of catalytic antibodies.

5. Experimental

5.1. General methods

All oxygen- or moisture-sensitive reactions were carried out under N_2. Analytical and preparative thin-layer chromatography was performed on silica gel 60 F_{254} plates (Merck). Flash chromatography was performed on silica gel 60 (230–240 mesh) (Merck). HPLC was performed on a Hitachi L-2130 system equipped with an L-2400 UV detector. ^{1}H and ^{13}C NMR spectra were taken on a JEOL NMR spectrometer. Chemical shifts (δ) are reported in ppm downfield from tetramethylsilane. Mass spectral data were collected with electrospray ionization (ESI) and electron ionization (EI) mass spectrometers.

5.2. Preparation of aldol products

5.2.1. Compounds 12, *syn*-12a, and *anti*-12a

To a solution of *p*-nitrobenzaldehyde (510 mg, 3.37 mmol) in 6 mL 2-butanone was added 600 μL of a 1% (w/v) aqueous NaOH solution at 0 °C. Stirring was continued for 19 h at 0 °C. The reaction mixture was then neutralized by addition of 1 M aqueous HCl and concentrated in vacuo. The residue was extracted with ether. The combined organic layers were dried over $MgSO_4$, filtered, and concentrated in vacuo. The residue was purified by HPLC (YMC-Pack ODS-AM AM323: C-18 reverse-phase column, φ 10 mm × 250 mm, acetonitrile/aqueous TFA (0.1%, 25:75), 3.0 mL/min, 254 nm, t_R: **12** = 44.0 min, **12a** (*syn* and *anti* mixture) = 38.5 min to give **12** as a white powder (193 mg, 26%) and **12a** (*syn* and *anti* mixture) as a white powder (242 mg, 32%). The *syn* and *anti* mixture **12a** was continuously purified by HPLC (YMC-Pack ODS-AM AM323: C-18 reverse-phase column, φ 10 mm × 250 mm, acetonitrile/aqueous TFA (0.1%, 20:80), 3.0 mL/min, 254 nm, t_R: *syn*-**12a** = 62.9 min, *anti*-**12a** = 66.0 min). **12**: ^{1}H NMR (400 MHz, $CDCl_3$): δ 8.21 (d, J = 8.8 Hz, 2H), 7.54 (d, J = 8.8 Hz, 2H), 5.27 (dd, J = 4.0 Hz, 8.1 Hz, 1H), 2.81–2.84 (m, 2H), 2.49 (q, J = 7.3 Hz, 2H), 1.09 (t, J = 7.3 Hz, 3H). *syn*-**12a**: ^{1}H NMR (400 MHz, $CDCl_3$): δ 8.22 (d, J = 8.8 Hz, 2H), 7.51 (d, J = 8.8 Hz, 2H), 5.28 (d, J = 2.7 Hz, 1H), 2.83 (qd, J = 2.7 Hz, 7.3 Hz, 1H), 2.25 (s, 3H), 1.05 (d, J = 7.3 Hz, 3H). *anti*-**12a**: ^{1}H NMR (400 MHz, $CDCl_3$): δ 8.22 (d, J = 8.8 Hz, 2H), 7.52 (d, J = 8.8 Hz, 2H), 4.87 (d, J = 7.3 Hz, 1H), 2.91 (quin, J = 7.3 Hz,1H), 2.21 (s, 3H), 1.03 (d, J = 7.3 Hz, 3H). **12**, LRMS (EI): m/z calcd for $C_{11}H_{13}NO_4$, 223.08; found, 223. **12a**, LRMS (EI): m/z calcd for $C_{11}H_{13}NO_4$, 223.08; found, 223.

5.2.2. Compound 13

2-Pentanone (110 μL, 1.0 mmol) was added to a freshly prepared solution of LDA (10% (w/w) suspension in hexanes; 3.1 mL, 2.2 mmol) in 5 mL of THF at −78 °C. After stirring at −78 °C for 30 min, a solution of *p*-nitrobenzaldehyde (151 mg, 1.0 mmol) in THF (5 mL) was added over a period of 1 min. After stirring at −78 °C for 3 h, saturated NH4Cl solution was added, and the reaction mixture was allowed to warm to room temperature. The product was extracted with ethyl acetate, dried over MgSO4, and evaporated in vacuo. The residue was purified by silica gel column chromatography (1:4 to 3:7 EtOAc/hexane) to afford compound **13** as a yellow solid (105 mg, 58%). ^{1}H NMR (400 MHz, $CDCl_3$): δ 8.22 (d, J = 8.8 Hz, 2H), 7.54 (d, J = 8.8 Hz, 2H), 5.25–5.29 (m, 1H), 3.64 (d, J = 3.2 Hz, 1H), 2.75–2.86 (m, 2H), 2.43 (t, J = 7.3 Hz, 2H), 1.63 (sext, J = 7.3 Hz, 2H), 0.93 (t, J = 7.3 Hz, 3H); LRMS (EI): m/z calcd for $C_{12}H_{15}NO_4$, 237.10; found, 237.

5.2.3. Compounds *syn*-13a and *anti*-13a

To a solution of *p*-nitrobenzaldehyde (200 mg, 1.32 mmol) in 3 mL of 2-pentanone was added 500 μL of a 1% (w/v) aqueous NaOH solution at 0 °C. Stirring was continued at 0 °C for 15 h. The reaction mixture was then neutralized by addition of 1 M aqueous HCl and concentrated in vacuo. The residue was extracted with ethyl acetate. The combined organic layers were dried over $MgSO_4$, filtered, and concentrated in vacuo. The residue was purified by HPLC (YMC-Pack ODS-AM AM323: C-18 reverse-phase column, φ 10 mm × 250 mm, acetonitrile/aqueous TFA (0.1%, 35:65),

3.0 mL/min, 254 nm, t_R: *syn*-**13a** = 24.8 min, *anti*-**13a** = 26.6 min) to give *syn*-**13a** as a white powder (59 mg, 19%) and *anti*-**13a** as a white powder (74 mg, 24%). *syn*-**13a**: ^{1}H NMR (400 MHz, $CDCl_3$): δ 8.21 (d, J = 8.8 Hz, 2H), 7.53 (d, J = 8.8 Hz, 2H), 5.10 (d, J = 4.4 Hz, 1H), 2.83 (dt, J = 4.4 Hz, 8.8 Hz, 1H), 2.17 (s, 3H), 1.68–1.79 (m, 1H), 1.53–1.63 (m, 1H), 0.85 (t, J = 7.3 Hz, 3H). *anti*-**13a**: ^{1}H NMR (400 MHz, $CDCl_3$): δ 8.22 (d, J = 8.8 Hz, 2H), 7.51 (d, J = 8.8 Hz, 2H), 4.92 (d, J = 6.8 Hz, 1H), 2.86 (dt, J = 6.8 Hz, 7.6 Hz, 1H), 2.13 (s, 3H), 1.58–1.69 (m, 1H), 1.43–1.54 (m, 1H), 0.91 (t, J = 7.0 Hz, 3H); LRMS (EI): m/z calcd for $C_{12}H_{15}NO_4$, 237.10; found, 237.

5.2.4. Compounds 14, *syn*-14a, and *anti*-14a

2-Hexanone (124 μL, 1.0 mmol) was added to a freshly prepared solution of LDA (10% (w/w) suspension in hexanes; 3.1 mL, 2.2 mmol) in 3 mL of THF at −78 °C. After stirring at −78 °C for 30 min, *p*-nitrobenzaldehyde (151 mg, 1.0 mmol), dissolved in 5 mL of THF, was added over a period of 1 min. After stirring for 3 h at −78 °C, saturated NH_4Cl solution was added, and the reaction mixture was allowed to warm to room temperature. The product was extracted with ethyl acetate, dried over $MgSO_4$, and evaporated in vacuo. The residue was purified by HPLC (YMC-Pack ODS-AM AM323: C-18 reverse-phase column, φ 10 mm × 250 mm, acetonitrile/aqueous TFA (0.1%, 35:65), 3.0 mL/min, 254 nm, t_R: **14** = 61.9 min, *syn*-**14a** = 42.4 min, and *anti*-**14a** = 44.5 min) to give **14** as a white powder (41 mg, 20%), *syn*-**14a** as a colorless oil (5.7 mg, 3%), and *anti*-**14a** (4.6 mg, 2%) as a colorless oil. Compound **14**: ^{1}H NMR (400 MHz, $CDCl_3$): δ 8.21 (d, J = 8.8 Hz, 2H), 7.54 (d, J = 8.8 Hz, 2H), 5.26–5.28 (m, 1H), 3.65 (d, J = 2.8 Hz, 1H), 2.76–2.87 (m, 2H), 2.45 (t, J = 7.6 Hz, 2H), 1.55–1.62 (m, 2H), 1.32 (sext, J = 7.6 Hz, 2H), 0.91 (t, J = 7.6 Hz, 3H). *syn*-**14a**: ^{1}H NMR (400 MHz, $CDCl_3$): δ 8.21 (d, J = 8.8 Hz, 2H), 7.52 (d, J = 8.8 Hz, 2H), 5.09 (d, J = 4.4 Hz, 1H), 3.24 (br s, 1H), 2.88 (dt, J = 4.4 Hz, 8.8 Hz, 1H), 2.18 (s, 3H), 1.62–1.68 (m, 1H), 1.42–1.51 (m, 1H), 1.25–1.28 (m, 1H), 1.09–1.13 (m, 1H), 0.82 (t, J = 7.3 Hz, 3H). *anti*-**14a**: ^{1}H NMR (400 MHz, $CDCl_3$): δ 8.22 (d, J = 8.8 Hz, 2H), 7.51 (d, J = 8.8 Hz, 2H), 4.90 (d, J = 6.6 Hz, 1H), 2.91–2.96 (m, 1H), 2.12 (s, 3H), 1.25–1.63 (m, 4H), 0.88 (t, J = 7.2 Hz, 3H). **14**, LRMS (EI): m/z calcd for $C_{13}H_{17}NO_4$, 251.28; found, 251. **14a**, LRMS (EI): m/z calcd for $C_{13}H_{17}NO_4$, 251.28; found, 251.

5.2.5. Compounds 15, *syn*-15a, and *anti*-15a

4-Hydroxy-2-butanone (110 μL, 1.1 mmol) was added to a freshly prepared solution of LDA (10% (w/w) suspension in hexanes; 3.1 mL, 2.2 mmol) in 3 mL of THF at −78 °C. After stirring at −78 °C for 30 min, a solution of *p*-nitrobenzaldehyde (151 mg, 1.0 mmol) in THF (5 mL) was added over a period of 1 min. After stirring at −78 °C for 3 h, saturated NH_4Cl solution was added, and the reaction mixture was allowed to warm to room temperature. The product was extracted with ethyl acetate, dried over MgSO4, and evaporated in vacuo. The residue was purified by silica gel column chromatography (EtOAc) to afford compound **15** as a pale yellow oil (13 mg, 6%). The *syn* and *anti* mixture **15a** was continuously purified by HPLC (YMC-Pack ODS-AM AM323: C-18 reverse-phase column, φ 10 mm × 250 mm, acetonitrile/aqueous TFA (0.1%, 35:65), 3.0 mL/min, 254 nm, t_R: *syn*-**15a** = 18.4 min, *anti*-**15a** = 15.9 min) to afford *syn*-**15a** as a pale yellow oil (5 mg, 2%) and *anti*-**15a** as a pale yellow oil (14 mg, 6%). Compound **15**: ^{1}H NMR (400 MHz, $CDCl_3$): δ 8.22 (d, J = 8.5 Hz, 2H), 7.55 (d, J = 8.5 Hz, 2H), 5.29–5.35 (m, 1H), 3.89–3.94 (m, 1H), 3.85 (q, J = 6.1 Hz, 1H), 3.41 (d, J = 4.0 Hz, 1H), 2.87–2.90 (m, 2H), 2.69–2.75 (m, 2H). *syn*-**15a**: ^{1}H NMR (400 MHz, $CDCl_3$): δ 8.25 (d, J = 8.8 Hz, 2H), 7.56 (d, J = 8.8 Hz, 2H), 5.50–5.53 (m, 1H), 4.01 (dd, J = 3.7 Hz, 12.2 Hz, 1H), 3.82 (dd, J = 3.7 Hz, 12.2 Hz, 1H), 3.79 (br s, 1H), 2.90 (q, J = 3.7 Hz, 1H), 2.68 (br s, 1H), 2.29 (s, 3H). *anti*-**15a**: ^{1}H NMR (400 MHz, $CDCl_3$): δ 8.24 (d, J = 8.8 Hz, 2H), 7.59 (d, J = 8.8 Hz, 2H), 5.23 (d, J = 6.4 Hz, 1H), 3.93 (dd, J = 4.1 Hz, 11.2 Hz, 1H), 3.71 (dd, J = 11.2 Hz, 4.8 Hz, 1H), 3.06–3.09 (m, 1H), 2.19 (s, 3H). **15**, LRMS (ESI^-): $[M-H]^-$ calcd for $C_{11}H_{12}NO_4$, 238.07; found, 238. **15a**, LRMS (ESI^-): $[M-H]^-$ calcd for $C_{11}H_{12}NO_4$, 238.07; found, 238.

5.2.6. Compounds *syn*-16 and *anti*-16

To a solution of *p*-nitrobenzaldehyde (151 mg, 1.0 mmol) in 1 mL of cyclobutanone was added 300 μL of a 1% (w/v) aqueous NaOH solution at 0 °C. Stirring was continued at 0 °C for 15 min. The reaction mixture was then neutralized by addition of 1 M aqueous HCl. The mixture was extracted with EtOAc. The combined organic layers were dried over $MgSO_4$, filtered, and concentrated in vacuo. The residue was purified by HPLC (YMC-Pack ODS-AM AM323:C-18 reverse-phase column, φ 10 mm × 250 mm, acetonitrile/aqueous TFA (0.1%, 35:65), 3.0 mL/min, 254 nm, t_R: *syn*-**16** = 14.7 min, *anti*-**16** = 16.5 min) to give *syn*-**16** as a colorless oil (26 mg, 12%) and *anti*-**16** as a white powder (60 mg, 27%). *syn*-**16**: ^{1}H NMR (400 MHz, $CDCl_3$): δ 8.22 (d, J = 8.8 Hz, 2H), 7.53 (d, J = 8.8 Hz, 2H), 5.30 (d, J = 3.4 Hz, 1H), 3.66–3.72 (m, 1H), 2.96–3.06 (m, 2H), 2.19–2.24 (m, 1H), 1.89–2.01 (m, 1H). *anti*-**16**: ^{1}H NMR (400 MHz, $CDCl_3$): δ 8.23 (d, J = 8.8 Hz, 2H), 7.56 (d, J = 8.8 Hz, 2H), 5.00 (d, J = 8.1 Hz, 1H), 3.58–3.65 (m, 1H), 3.09–3.18 (m, 1H), 2.94–3.04 (m, 1H), 2.07–2.17 (m, 1H), 1.88–1.98 (m, 1H); LRMS (ESI^-): $[M-H]^-$ calcd for $C_{11}H_{10}NO_4$, 220.06; found, 220.

5.3. Preparation of antibody 27C1

Hybridoma cells for antibody 27C1 were grown to 4 L, and the supernatants were purified by anti-mouse IgG + IgM affinity chromatography (CHROMATOP) (NGK, loaded in PBS and eluted with 0.2 M Gly-HCl pH 2.5) to yield purified antibody.

5.4. Antibody assays for cross-aldol reactions

All antibody-catalyzed or background reactions were performed in 50 mM Tris–HCl pH 8.0 at 25 °C. The reaction products were monitored by HPLC. The analytical HPLC was performed on a Hitachi L-2130 unit equipped with a Hitachi L-2400 UV detector using a YMC-Pack ODS-AM AM303 column (250 × 4.6 mm) and acetonitrile/water mixtures (containing 0.1% TFA) as eluent at a flow rate of 1.0 mL/min.

5.4.1. Specific rates of aldol reactions

The specific rates of cross-aldol reactions were determined before 10% completion of the reactions using 1 mM acceptor substrate **4**, 5% donor ketones, 10 mM primary amine **2**, and 10 μM antibody. The specific rate for the cross-aldol reaction of 2-hexanone and *p*-nitrobenzaldehyde was determined with 2.5 mM **2**. All kinetic assays were measured in duplicate.

5.4.2. Regioselectivity of cross-aldol reactions

The regioselectivity of antibody-catalyzed cross-aldol reactions was determined before 10% completion of the reactions using 500 μM acceptor substrate **4**, 5% donor ketones, 500 μM primary amine **2**, and 10 μM antibody. The uncatalyzed reactions were performed under the same conditions except for the absence of antibody. The reactions were incubated for 24 h. The ratios of isomers were determined by HPLC analysis. The conversion rates of the uncatalyzed reactions were estimated to be 73% (2-butanone), 19% (2-pentanone), 29% (2-hexanone), and 58% (4-hydroxy-2-butanone). All kinetic assays were measured in duplicate.

5.4.3. Determination of enantiomeric excess of an aldol product 12

The enantiomeric excess (ee) of **12** catalyzed by 27C1 was determined under the following conditions: 0.5 mM *p*-nitrobenzaldehyde **4**, 5% 2-butanone, 0.5 mM primary amine **2**, and 20 μM

antibody in 50 mM Tris–HCl pH 8.0. Total DMSO concentration was kept at 4%. The reaction mixture was incubated at 25 °C for 2 h. The reaction mixture was purified by HPLC (YMC-Pack ODS-AM AM323: C-18 reverse-phase column, φ 10 mm × 250 mm, acetonitrile/aqueous TFA (0.1%, 25:75), 3.0 mL/min, 254 nm, t_R: **12** = 44.0 min, **12a** (*syn* and *anti* mixture) = 38.5 min to give pure aldol product **12**. The aldol product was redissolved in 2-propanol and the ee was determined by normal phase HPLC using Daicel column (CHIRALPAK AS-H, φ 4.6 mm × 250 mm, 2-propanol/hexane (50:50), 0.5 mL/min, 275 nm, t_R: (*R*)-**12** = 12.5 min and (*S*)-**12** = 16.8 min). Chemically synthesized standard was prepared according to the literature procedure to provide (*R*)-**12**.[35] Briefly, to a mixture of anhydrous DMSO (4 mL) and 2-butanone (1 mL) was added *p*-nitrobenzaldehyde (100 mg, 0.66 mmol) followed by L-Proline (20 mol %) and the resulting mixture was stirred at room temperature for 4 h. The reaction mixture was treated with saturated ammonium chloride solution, the layers were separated, and the aqueous layer was extracted with EtOAc, dried over $MgSO_4$, and evaporated in vacuo. The residue was purified by flash chromatography (1:4 EtOAc/hexane) to give (*R*)-**12** as a yellow powder (66 mg, 53%). Chiral-phase HPLC analysis revealed that (*R*)-**12** was formed in 59% ee. The ^{1}H NMR, LRMS, and ee data were identical to the literature.[35]

5.5. Kinetic parameters determination of the decarboxylation reaction

The 27C1-catalyzed decarboxylation reaction was performed in a Digital Uni Ace UA-100 water bath (Eyela) at 25 °C (±0.1) in 50 mM Tris–HCl pH 8.0. In all experiments the total DMSO concentration was kept at 10%. The reaction was followed by monitoring the formation of (*p*-nitrophenyl)acetone by reversed-phase HPLC at 280 nm. The analytical HPLC was performed on a Hitachi L-2130 unit equipped with a Hitachi L-2400 UV detector, using a YMC-Pack ODS-AM AM303 column eluted with acetonitrile/aqueous TFA (0.1%, 60:40) at a flow rate of 1.0 mL/min. The kinetic parameters were caliculated for a rapid-equilibrium random system.[36] The antibody-catalyzed rates were measured at fixed concentrations of β-keto acid **3** ($0.5\ mM \leqslant [\mathbf{3}] \leqslant 3\ mM$) and varying concentrations of amine **2** ($1.5\ mM \leqslant [\mathbf{2}] \leqslant 10\ mM$). Final antibody concentration (5 μM) and temperature (25 °C) were maintained throughout the assay. Kinetic parameters were determined by a two-step analysis. First, Lineweaver–Burk ($1/V$ vs $1/S$) plots of the raw data were constructed. These *y*-intercepts and slopes were then replotted to yield the actual V_{max} and K_m (β-keto acid **3**) values for the 27C1-catalyzed process. The k_{cat} values were determined from the actual V_{max} values. Similarly, the antibody-catalyzed rates were measured at fixed concentrations of amine **2** ($1.5\ mM \leqslant [\mathbf{2}] \leqslant 10\ mM$) and varying concentrations of β-keto acid **3** ($0.5\ mM \leqslant [\mathbf{3}] \leqslant 3\ mM$). Analogous plots were constructed to provide kinetic constants for amine **2**. All kinetic assays were measured in duplicate.

Acknowledgement

This work was supported by JSPS KAKENHI Grant Number 16350091.

References and notes

1. Nelson, S. G. *Tetrahedron: Asymmetry* **1998**, *9*, 357.
2. Machajewski, T. D.; Wong, C.-H. *Angew. Chem., Int. Ed.* **2000**, *39*, 1352.
3. Notz, W.; Tanaka, F.; Barbas, C. F., III *Acc. Chem. Res.* **2004**, *37*, 580.
4. Gijsen, H. J. M.; Qiao, L.; Fitz, W.; Wong, C.-H. *Chem. Rev.* **1996**, *96*, 443.
5. Hamilton, G. A.; Westheimer, F. H. *J. Am. Chem. Soc.* **1959**, *81*, 6332.
6. Fridovich, I.; Westheimer, F. H. *J. Am. Chem. Soc.* **1962**, *84*, 3208.
7. Laursen, R. A.; Westheimer, F. H. *J. Am. Chem. Soc.* **1966**, *88*, 3426.
8. Takagi, W.; Guthrie, J. P.; Westheimer, F. H. *Biochemistry* **1968**, *7*, 905.
9. Autor, A. P.; Fridovich, I. *J. Biol. Chem.* **1970**, *245*, 5214.
10. Frey, P. A.; Kokesh, F. C.; Westheimer, F. H. *Biochemistry* **1971**, *14*, 7266.
11. Kokesh, F. C.; Westheimer, F. H. *J. Am. Chem. Soc.* **1971**, *93*, 7270.
12. Schmidt, D. E., Jr.; Westheimer, F. H. *Biochemistry* **1971**, *10*, 1249.
13. Westheimer, F. H. *Tetrahedron* **1995**, *51*, 3.
14. Westheimer, F. H. Proceedings of the Robert A. Welch Fundation Conferences on Chemical Research; Robert A. Welch Foundation, Huston, **1971**; Vol. 15, pp 7–50.
15. Kobes, R. D.; Dekker, E. E. *Biochem. Biophys. Res. Commun.* **1967**, *27*, 607.
16. Nishihara, H.; Dekker, E. E. *J. Biol. Chem.* **1972**, *247*, 5079.
17. Vlahos, C. J.; Dekker, E. E. *J. Biol. Chem.* **1986**, *261*, 11049.
18. Wangner, J.; Lerner, R. A.; Barbas, C. F., III *Science* **1995**, *270*, 1797.
19. Björnestedt, R.; Zhong, G.; Lerner, R. A.; Barbas, C. F., III *J. Am. Chem. Soc.* **1996**, *118*, 11720.
20. Hoffmann, T.; Zhong, G.; List, B.; Shabat, D.; Anderson, J.; Gramatikova, S.; Lerner, R. A.; Barbas, C. F., III *J. Am. Chem. Soc.* **1998**, *120*, 2768.
21. List, B.; Shabat, D.; Barbas, C. F., III; Lerner, R. A. *Chem. Eur. J.* **1998**, *4*, 881.
22. Sinha, S.; Barbas, C. F., III; Lerner, R. A. *Proc. Natl. Acad. Sci. U.S.A.* **1998**, *95*, 14603.
23. Sinha, S.; Sun, J.; Miller, G.; Barbas, C. F., III; Lerner, R. A. *Org. Lett.* **1999**, *1*, 1623.
24. Shabat, D.; List, B.; Lerner, R. A.; Barbas, C. F., III *Tetrahedron Lett.* **1999**, *40*, 1437.
25. Ishikawa, F.; Tsumuraya, T.; Fujii, I. *J. Am. Chem. Soc.* **2009**, *131*, 456.
26. Guthrie, J. P.; Jordan, F. *J. Am. Chem. Soc.* **1972**, *94*, 9132.
27. Guthrie, J. P.; Jordan, F. *J. Am. Chem. Soc.* **1972**, *94*, 9136.
28. Hine, J.; Via, F. A. *J. Am. Chem. Soc.* **1972**, *94*, 190.
29. O'Leary, M. J.; Baughn, R. L. *J. Am. Chem. Soc.* **1972**, *94*, 626.
30. Highbarger, L. A.; Gerlt, J. A.; Kenyon, G. L. *Biochemistry* **1996**, *35*, 41.
31. Kurihara, S.; Tsumuraya, T.; Suzuki, K.; Kuroda, M.; Liu, L.; Takaoka, Y.; Fujii, I. *Chem. Eur. J.* **2000**, *6*, 1656.
32. Miyashita, H.; Karaki, Y.; Kikuchi, M.; Fujii, I. *Proc. Natl. Acad. Sci. U.S.A.* **1993**, *90*, 5337.
33. Fujii, I.; Fukuyama, S.; Iwabuchi, Y.; Tanimura, R. *Nat. Biotechnol.* **1998**, *16*, 463.
34. Miyashita, H.; Hara, T.; Tanimura, R.; Fukuyama, S.; Cagnon, C.; Kohara, A.; Fujii, I. J. *Mol. Biol.* **1997**, *267*, 1247.
35. Sakthivel, K.; Notz, W.; Bui, T.; Barbas, C. F., III *J. Am. Chem. Soc.* **2001**, *123*, 5260.
36. Segal, I. H. *Enzyme Kinetics*; John Wiley & Sons, Inc.: New York, 1975.